

Electronic Supporting Information

Chain conformation near the buried interface in nanoparticle stabilized polymer thin films

Deborah A. Barkley¹, Naisheng Jiang², Mani Sen², Maya K. Endoh², Jonathan G. Rudick¹, Tadanori Koga^{1,2}, Yugang Zhang^{3,4}, Oleg Gang^{4,5}, Guangcui Yuan⁶, Sushil K. Satija⁶, Daisuke Kawaguchi⁷, Keiji Tanaka⁸, Alamgir Karim⁹

¹Department of Chemistry, Stony Brook University, Stony Brook, New York 11794-3400

²Department of Materials Science and Chemical Engineering, Stony Brook University, Stony Brook, New York 11794-2275

³National Synchrotron Light Source II, Brookhaven National Lab, Upton, NY 11973

⁴Center for Functional Nanomaterials, Brookhaven National Lab, Upton, NY 11973

⁵Department of Chemical Engineering and Applied Physics and Applied Mathematics, Columbia University, New York, NY 10027

⁶Center for Neutron Research, National Institute of Standards and Technology, Gaithersburg, MD 20899

⁷Education Center for Global Leaders in Molecular Systems for Devices, Kyushu University, Fukuoka 819-0395, Japan

⁸Department of Applied Chemistry, Faculty of Engineering, Kyushu University, Fukuoka 819-0395, Japan

⁹College of Polymer Science and Polymer Engineering, the University of Akron, Ohio 44325-0301

1. XPS results

The sample characterized using this technique was the PS50k/Au (0.1%) flattened layer. Hence, the presence of PS after rinsing with toluene is clearly indicated in the results by the C 1s peak at $E_{\text{binding}} = 285$ eV and the C π - π peak at $E_{\text{binding}} = 291$ - 293 eV. The presence of the Au nanoparticles (with dodecanethiol surfactant) is also indicated by the Au 4f5/2 peak at $E_{\text{binding}} = 91$ eV and the S 2p peak at $E_{\text{binding}} = 169$ eV.

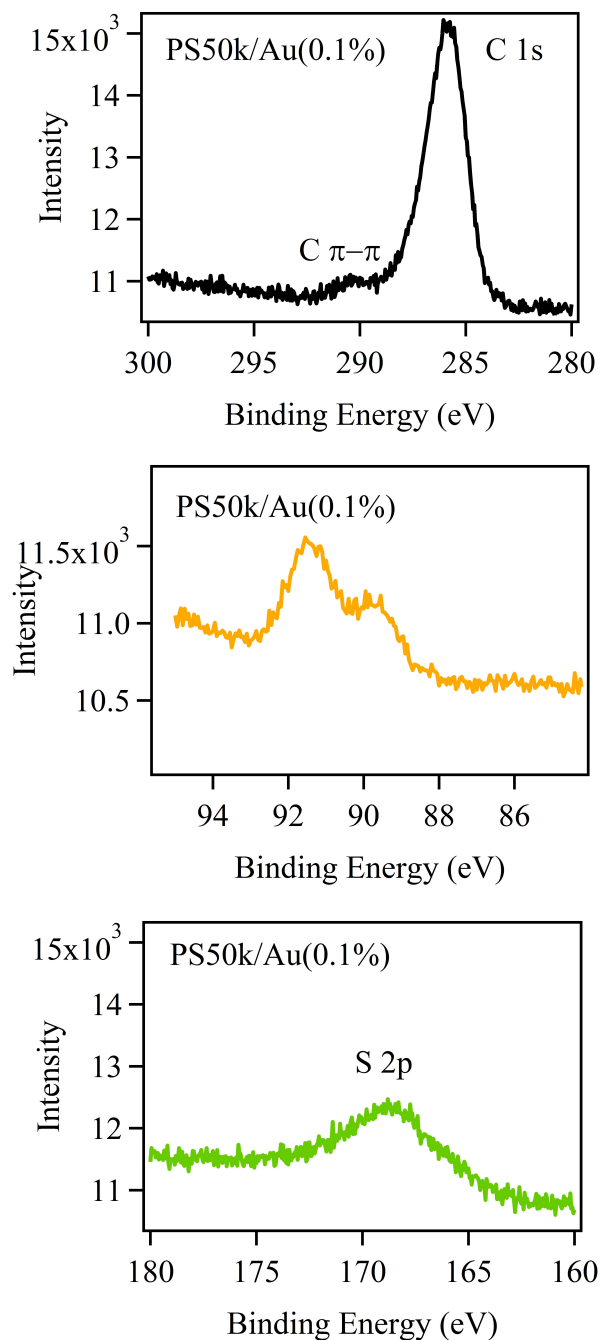


Fig. S1 X-ray photoelectron spectroscopic (a) C 1s narrow scan (b) Au 4f5/2 narrow scan and (c) S 2p narrow scan of the PS50k/Au(0.1%) residual layer.

2. AFM of the PS50k/Au flattened layers

Using free ImageJ software (<https://imagej.nih.gov/ij/>), the area fraction of nanoparticle clusters, the number of nanoparticle clusters, the average nanoparticle cluster radius (r), and the average distance between nanoparticle clusters (l), which was estimated as $\frac{\text{total image length}}{\sqrt{\text{number of clusters}}} = l$, were estimated from the AFM image of the PS50k/Au(0.05%) residual layer (Fig. S2). From these values, the volume fraction of the Au (ϕ) was calculated from the area fraction according to the following equation with the assumption that the gold NPs are spherical¹:

$$\phi = \left(\frac{4r}{3l}\right) \times (\text{area fraction}) \quad (\text{S2}).$$

| Au as cast % | AFM area fraction (%) | r (nm) | l (nm) | ϕ (%) |
|--------------|-----------------------|----------|----------|------------|
| 0.05 | 3.1 | 32 | 315 | 0.4 |
| 0.25 | 4.4 | 60 | 500 | 0.7 |

Table S1. Data analysis of the AFM images

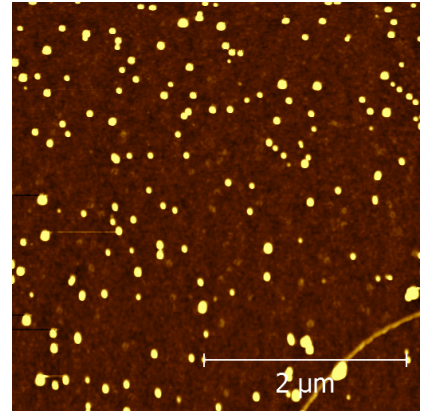


Fig. S2 AFM image of the PS/Au (0.05%) flattened layer.

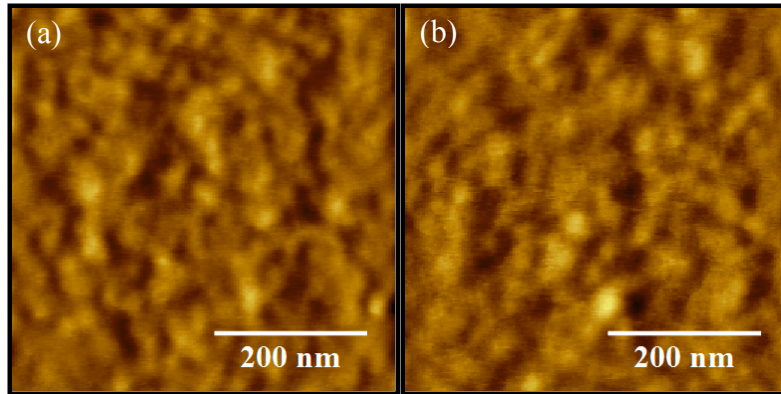


Fig. S3 Representative $0.5 \mu\text{m} \times 0.5 \mu\text{m}$ AFM height images of PS/Au adsorbed layers with (a) $\phi_{\text{Au}} = 0.05\%$ and (b) $\phi_{\text{Au}} = 0.25\%$. The AFM images are focused on the well-dispersed Au/polymer regions to avoid the disturbance of the large Au clusters on the morphology of the flattened chains, as shown in Fig. S2. Height scales of both images are 0 - 2 nm. It was found that the RMS roughness of the polymer region is independent of Au concentration with a value of 0.21 ± 0.05 nm. All the RMS roughness values were obtained using the Gwyddion image software with exactly same image size.

3. GISAXS results on the PS(50k)/Au(0.05%) flattened layer

Fig. S3 shows the GISAXS profiles for the PS(50k)/Au(0.05%) flattened layer at room temperature. From the figure, we can see a power law scattering profile given by $I(q) \sim q^{-3}$ in the nearly entire q -range used for the PS50k/Au (0.05%) flattened layer. This power law exponent indicates that the scattering is attributed to the interface of a randomly phase separated two-dimensional object (i.e., the gold nanoparticles migrated to the substrate surface)². Hence, the interparticle (or intercluster) spacing is expected to be more than 100 nm (i.e., the spatial resolution of the GISAXS technique). The comparison with Fig. 2d suggests that the inter particle spacing of the Au nanoparticles migrated to the substrate surface decreases with increasing the Au concentration.

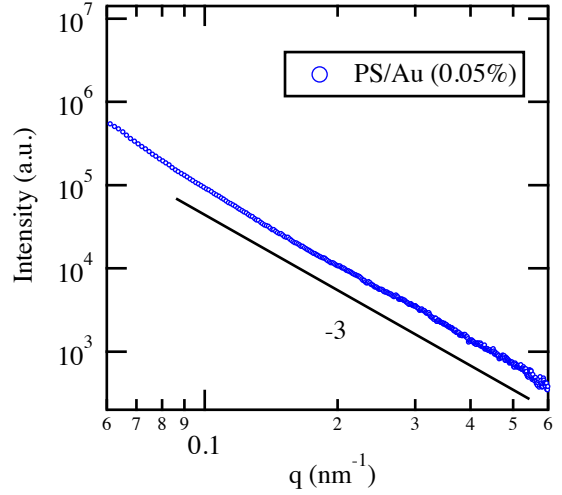


Fig. S4 GISAXS profile of the PS50k/Au (0.05%) flattened layer at room temperature.

4. Neutron Reflectivity results on the nanoparticle-free PS flattened layers

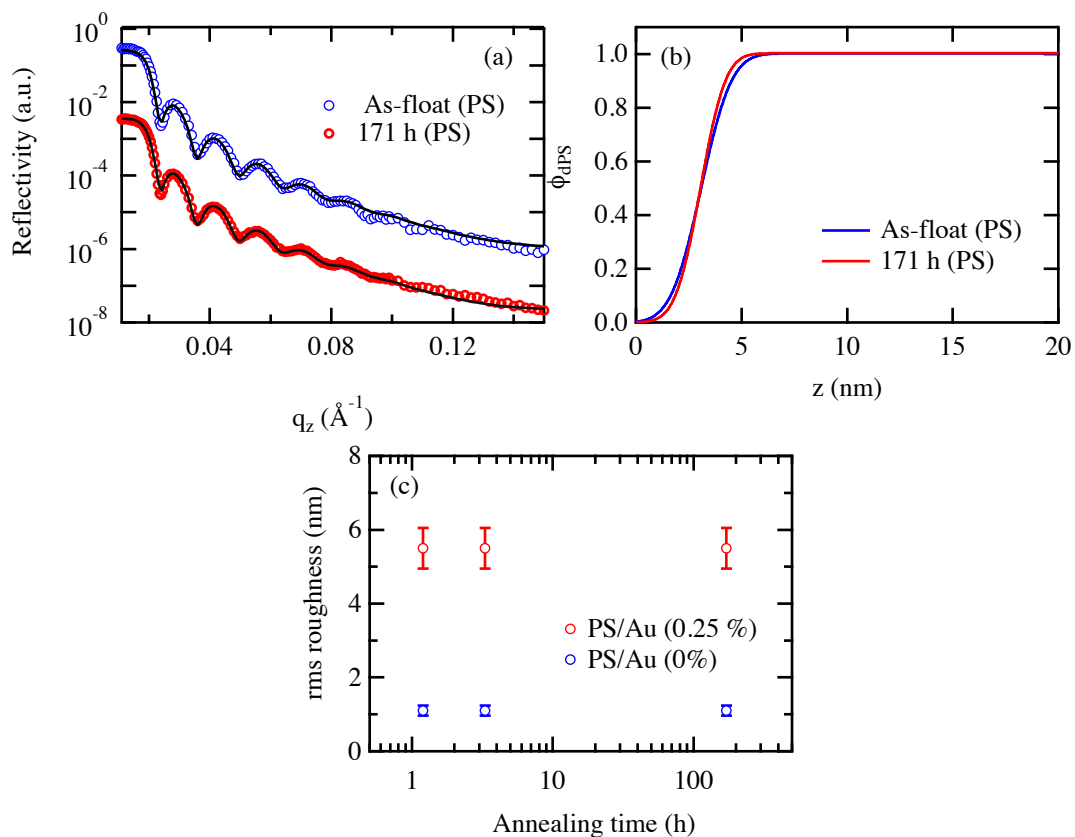


Fig. S5 NR results for the bilayer of the bottom PS50k and the top d-PS film annealed at 150 °C over the given annealing times. The solid lines in (a) are the best-fits to the data based on the volume fraction profiles of dPS (ϕ) shown in (b), respectively. The root-mean-square (rms) roughness values of the hPS/Au flattened layer/dPS overlayer and the hPS flattened layer/dPS overlayer via thermal annealing at $T=150$ °C are shown in (c).

5. Surface energy obtained from liquid contact angle measurements

In order to calculate the E_p value, we estimated the surface energies based on the static contact angle of three liquids for the Si and for a spin-coated layer of nanoparticles on the clean Si substrate. On the basis of the Young's equation ($\gamma_s = \gamma_l \cos \theta + \gamma_{sl}$) and the Owens-Wendt-Kaelble equation ($\gamma_{ls} = \gamma_l + \gamma_s - 2(\gamma_s^d \gamma_l^d)^{1/2} - 2(\gamma_s^p \gamma_l^p)^{1/2}$) (γ_s^d and γ_s^p are the dispersion and polar parts of the surface energy of the solid, γ_l^d and γ_l^p are the dispersion and polar parts of the surface energy of the liquid)³. Hence, $E_p = \gamma_{S-P} - \gamma_{S-N}$ (where γ_{S-P} and γ_{S-N} are the interfacial energy between the substrate and polymer and between the substrate and nanoparticles, respectively) was estimated to be $E_p = 20.4 \text{ mJ/m}^2 - 14.3 \text{ mJ/m}^2 = 6.1 \text{ mJ/m}^2$ for the PS/Au blend film on the Si substrate.

TABLE S2. Contact angles on the Au monolayers

| Au | γ | γ^d | γ^p | θ_{Au} |
|----------------|----------|------------|------------|---------------|
| water | 72.80 | 22.60 | 50.20 | 76.40 |
| glycerol | 63.40 | 37.00 | 26.40 | 55.04 |
| 1,4-butanediol | 44.00 | 24.00 | 20.00 | 22.67 |

TABLE S3. Surface tension of the components

| Component | Surface tension (mJ/m ²) | | |
|-----------------|--------------------------------------|------------|------------|
| | γ | γ^d | γ^p |
| Si ⁴ | 51.6 | 25.8 | 25.8 |
| PS ⁵ | 42.0 | 41.4 | 0.6 |
| Au NPs | 50.3 | 47.27 | 3.04 |

| γ_{BSi-PS} | γ_{BSi-Au} | γ_{PS-Au} | E_p |
|------------------------|------------------------|------------------------|-----------------------|
| 20.4 mJ/m ² | 14.3 mJ/m ² | 1.12 mJ/m ² | 6.1 mJ/m ² |

TABLE S4. Surface energies of components (mJ/m²)

| γ_{Au-Air} | γ_{PS-Air} |
|-------------------|-------------------|
| 89.72 | 90.08 |

References

- Farmer, J.; Duong, B.; Seraphin, S.; Shimpalee, S.; Martínez-Rodríguez, M. J.; Van Zee, J. W. Assessing porosity of proton exchange membrane fuel cell gas diffusion layers by scanning electron microscope image analysis. *J. Power Sources* **2012**, 197, 1-11.
- Debye, P.; Bueche, A. M. Scattering by an inhomogeneous solid. *J. Appl. Phys.* **1949**, 20, (6), 518-525.
- Kwok, D. Y.; Neumann, A. W. *Adv. Colloid Interface Sci.* **1999**, 81, 167-249.

4. Kawai, A.; Kawakami, J.; Sasazaki, H. Surface energy change of Si(100) wafer by exposing to air. *J. Photopolym. Sci. Technol.* **2008**, 21, 739-740.
5. Owens, D. K.; Wendt, R. C. Estimation of the surface free energy of polymers. *J. Appl. Polym. Sci.* **1969**, 13, 1741-1747.